

Squeeze flow modeling with the use of micropolar fluid theory

A. KUCABA-PIĘTAL*

Department of Fluid Mechanics, Rzeszów University of Technology, 8 Powstańców Warszawy St., 35-959 Rzeszów, Poland

Abstract. The aim of this paper is to study the applicability of micropolar fluid theory to modeling and to calculating tribological squeeze flow characteristics depending on the geometrical dimension of the flow field. Based on analytical solutions in the lubrication regime of squeeze flow between parallel plates, calculations of the load capacity and time required to squeeze the film are performed and compared – as a function of the distance between the plates – for both fluid models: the micropolar model and the Newtonian model. In particular, maximum distance between the plates for which the micropolar effects of the fluid become significant will be established. Values of rheological constants of the fluids, both those experimentally determined and predicted by means of using equilibrium molecular dynamics, have been used in the calculations. The same analysis was performed as a function of dimensionless microstructural parameters.

Key words: micropolar fluid, squeeze flow, MEMS, tribology, non-Newtonian fluid.

1. Introduction

Squeeze flow between parallel plates is an important area of study because of its many industrial and practical applications. These include MEMS devices (such as squeeze film damping), polymer process industry, automotive components, squeeze films in power transmissions and journal bearing.

Since Reynolds in 1886, many researchers have contributed their efforts towards solving this problem in different geometries. Squeeze film problems have been solved using the Newtonian fluid model [1, 2] as well as the micropolar fluid model [3–8]. Several investigators have found some advantages of the micropolar fluid model over the Newtonian fluid model, such as an increased load-carrying capacity and an increased approaching time for squeeze films, which has been observed experimentally. This happened in two cases: either when small amounts of long-chain polymer solutions were added to Newtonian fluids operating as lubricants or when very thin films were squeezed. In such situations, the small height of the gap between squeezing plates implies the dominance of the surface forces over the volume forces. The surface forces eccentrically influence the fluid molecules, causing them to rotate (or spin). This effect – which is not possible to model within the frame of the classical continuum medium (Cauchy) theory – can be observed in particular during the squeeze flow of polyatomic molecule liquids (bioliquids, polar liquids), liquids with additives or particles (nanofluids) as well as in the case of flow through a very narrow channel.

Micropolar fluid theory (MFT), derived by Eringen within the framework of extended continua is based on the assumption of a continuous medium but also takes into account the micro-

rotation of molecules (microrotation – the spinning motion of molecules independent of the rotation of flow velocity field).

MFT is being widely developed due to its potential use in tribology, microdevices, biotribology, and magnetorheology, to describe the flows in microchannels [10–12]. For the past twenty years, significant progress and results supporting the usefulness of MFT to model fluid flow in narrow gaps and passages have been developed. Based on the molecular dynamics method, it was confirmed that during the Poiseuille flow in very narrow channels, the microrotation velocity – not included in the classical continuum theory – does in fact exist and those results are sufficiently consistent with the results obtained based on the analytical solution of the micropolar fluid flow [13–17]. A new method has been developed by Hansen et al. [18] for designating the micropolar viscosity coefficients for real fluids using equilibrium molecular dynamics and values for water have been presented in the same work.

Research on scale effect of MFT applicability to microflows modeling started in 2004. It showed that micropolar fluid equations of motion are being reduced to their counterparts in the classical continuum medium (Cauchy) theory, i.e. the Navier–Stokes equations, when the characteristic linear dimension of the flow field is sufficiently large [15, 16]. As a result, questions concerning the size of the flow field arose as concerns the effective use of MFT in solving flow problems. Hagen–Poiseuille fluid flow in this context was studied in detail [16] and a microchannel maximum diameter value, above which the effect of micropolarity is negligibly small, was calculated for some real fluids, including water and blood, and expressed in dimensionless micropolar parameters. Hoffmann et al. (2007) compared the resistance force exerted on a sphere moving in micropolar fluids: water and blood, and showed that deviations are being observed only for small sphere radii.

Lubrication-type analysis for squeezing flow is well established, and physical effects such as increased load capacity, etc., have been known since the 1970s, quoted e.g. in [3, 4]. The increasing number of articles regarding squeeze flow prob-

*e-mail: anpietal@prz.edu.pl

Manuscript submitted 2016-12-29, initially accepted for publication 2017-03-28, published in December 2017.

lems was the motivation behind undertaking the study presented herein. The goal of this paper is to answer the question of what the limiting value of the gap height between squeezing plates is, below which the micropolar effects of the fluid flow are visible and cannot be neglected, i.e. MFT should be applied.

To answer this question, quantitative evaluation is performed of the influence of coupled stresses in a micropolar fluid on the squeezing fluid flow characteristics as a function of the distance between the plates. On the basis of classic results of analytical solutions for squeeze flow problems, when the considered system is within the lubrication regime, load supporting capacity and squeeze time are both evaluated. To assess the “micropolar effects”, the ratio between the load capacity of the micropolar and Newtonian fluids as a function of the distance, h , was introduced. The comparison was obtained using available data for the physical parameters of individual fluids considered in [15, 16] it was showed showed that the discrepancies are visible only for very small values of the gap.

Results obtained in the paper give new insight into practical MFT application and contribute to effective squeeze flow micropolar fluid modeling:

- 2) they demonstrate that the impact of micropolar properties of the fluid on tribological squeeze flow characteristics is limited only to certain “maximum” distance h_{max} between squeezed plates,
- 3) they show that the distance h_{max} reflects the inner structure of the fluid and can be defined by micropolar fluid viscosity coefficients, which describe fluid rheological properties,
- 4) they indicate that the calculations of the squeeze film characteristics for both the micropolar fluid and the Newtonian fluid models are the same for distances greater than h_{max} ,
- 5) they allow for calculation of distance values h_{max} for micropolar fluids; for several fluid considered in the paper, including inter alia water, the h_{max} value is given.

The paper is organized as follows. In Section 2, the micropolar fluid model is presented. In Section 3, flow problems are described, and the results are presented in Section 4. The study’s conclusions are presented in Section 5.

2. Micropolar field equation

2.1. Constitutive equations. The most important feature of MFT is the utilization of two tensors, the non-symmetric stress tensor T , and the couple stress tensor C . The constitutive equations for a micropolar fluid [9], where the stress tensor $T = \{T_{ij}\}$ is a non-symmetric tensor and the couple stress tensor $C = \{C_{ij}\}$, are as follows:

$$T_{ij} = (-p + \lambda V_{k,k})\delta_{ij} + \mu(V_{i,j} + V_{j,i}) + \kappa(V_{j,i} - \varepsilon_{ijk}\omega_k) \quad (1)$$

$$C_{ij} = \alpha\omega_{k,k}\delta_{ij} + \beta\omega_{i,j} + \gamma\omega_{j,i} \quad (2)$$

where the symbols denote: p – pressure, ω – the microrotation field with $\omega = (\omega_1, \omega_2, \omega_3)$, V – the velocity field with $V = (V_1, V_2, V_3)$, λ , μ and κ – coefficients of bulk, shear and vortex (or rotational) viscosities, respectively, α , β and γ – coef-

ficients of spin gradient viscosities, ε_{ijk} – the Levi-Civita tensor, and δ_{ik} – the Kronecker delta function.

The viscosity coefficients satisfy the following inequalities [9]:

$$\begin{aligned} \kappa > 0.3\lambda + \kappa + 2\mu > 0.2\mu + \kappa > 0 \\ 3\alpha + 2\gamma > 0, -\gamma < \beta < \gamma, \gamma > 0 \end{aligned}$$

An alternative form to (1) is the following:

$$T_{ij} = (-p + \lambda V_{k,k})\delta_{ij} + (\mu + \kappa/2)(V_{i,j} + V_{j,i}) + \kappa(V_{j,i} - V_{i,j}) - \kappa\varepsilon_{ijk}\omega_k \quad (3)$$

and the symmetric part of the stress tensor T expression in (3) is:

$$T_{ij}^{[S]} = (-p + \lambda V_{k,k})\delta_{ij} + (\mu + \kappa/2)(V_{i,j} + V_{j,i}). \quad (4)$$

This form is the same as the definition of the stress tensor in classical hydrodynamics, where $\mu_N = \mu + \kappa/2$ denotes the dynamic Newtonian viscosity coefficient.

2.2. Flow equations. In the most general form [9, 19], the micropolar field equations for an incompressible fluid representing conservation laws are the following:

conservation of mass:

$$\text{div} V = 0 \quad (5)$$

conservation of linear momentum

$$\rho \frac{dV}{dt} = \rho f - \text{grad} p - (\mu + \kappa)\text{rot rot} V + \kappa \text{rot} \omega \quad (6)$$

conservation of angular momentum

$$\begin{aligned} \rho I \frac{d\omega}{dt} = (\alpha + \beta + \gamma)\text{grad div} \omega - \gamma \text{rot rot} \omega + \\ + \kappa \text{rot} V - 2\kappa \omega + \rho g \end{aligned} \quad (7)$$

where: ρ is the density, f is the body force per unit mass with $f = (f_1, f_2, f_3)$, g is the body torque per unit mass with $g = (g_1, g_2, g_3)$, and I is the microinertia coefficient.

The boundary conditions for the velocity field are the same as in the classic case with no slip conditions. For the microrotation, the Dirichlet boundary condition ($\omega = 0$) or the dynamic boundary condition is often used (see [19–21]). The last one, in the form of $\omega = \alpha \text{rot} V$, $0 < \alpha < 1$, will be used in this paper.

2.3. Dimensionless parameters. In addition to the usual dimensionless numbers encountered in classical hydrodynamics, the micropolar fluid flow is characterized by two dimensionless numbers, N and L

$$N = \sqrt{\frac{\kappa}{2\mu_N + \kappa}}, \quad L = \frac{L_c}{l}, \quad l = \sqrt{\frac{\gamma}{4\mu_N}}. \quad (8)$$

The dimensionless parameter N characterizes a coupling between the coefficients of rotational viscosity, κ , and shear

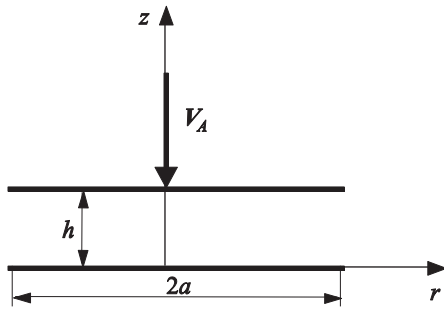


Fig. 1. Squeeze film configuration

viscosity, μ , i.e. $0 \leq N \leq 1$ [9]. The L parameter characterizes an interaction of flow geometry and the fluid properties, where L_c denotes the characteristic linear dimension of the flow field and the l parameter has a dimension of length and characterizes the relative length of the fluid microstructure. In general terms, the larger the molecules, the larger the value of the parameter l [22, 23] and elsewhere).

For a given fluid, the value of the N parameter is constant, but the L parameter depends explicitly on the geometry of the flow L_c since l is a constant for a given fluid.

3. Problem formulation

We studied the quasi-stationary two-dimensional Stokes flow of an incompressible micropolar fluid between two closely spaced parallel circular plates (Fig. 1). The upper plate moves with velocity V_A towards the stationary lower plate.

In the cylindrical coordinate system (r, θ, z) , we denoted the components of the velocity vector by $V = (V_r(r, z), 0, V_z(r, z))$, microrotation $\omega = (0, \omega(r, z), 0)$, and pressure $p(r, z)$. The lower plate was located at $z = 0$ and the upper plate at $z = h$, with the plate diameter being equal to $2a$. The translational velocity of the plate is $V_A = (0, 0, -U)$. We restricted our attention to fluid flow in the gap between the plates, with the vector of the mass moment $g = 0$, mass force $f = 0$, and the gap height h defined as the distance between the parallel plates being sufficiently small, i.e. $h/a \ll 1$, and $V_z \ll V_r$. This permitted us to make considerable simplifications of the fluid flow equation (6), which was transformed to a form (derived in [4]) which, together with the continuity equation, reads as follows:

$$\left. \begin{aligned} \rho \frac{\partial p}{\partial r} &= \frac{1}{2}(2\mu_N + \kappa) \frac{\partial^2 V_r}{\partial z^2} + \kappa \frac{\partial \omega}{\partial z} \\ \rho \gamma \frac{\partial^2 \omega}{\partial z^2} - 2\kappa \omega - \kappa \frac{\partial V_r}{\partial z} &= 0 \\ \frac{\partial p}{\partial z} &= 0 \\ \frac{1}{r} \frac{\partial}{\partial r}(rV_r) + \frac{\partial}{\partial z} V_z &= 0 \end{aligned} \right\} \quad (9)$$

The boundary conditions imposed onto the velocity and microrotation vectors on the plates have the following form:

$$V_r = 0, \quad V_z = -U \quad \text{for } z = h \quad (10)$$

$$V_r = 0, \quad V_z = 0 \quad \text{for } z = 0 \quad (11)$$

$$\left. \begin{aligned} \omega &= \frac{1}{2} \alpha_0 \text{rot } V \quad \text{for } z = h \\ \omega &= \frac{1}{2} \alpha_0 \text{rot } V \quad \text{for } z = 0 \end{aligned} \right\} \quad (12)$$

where α_0 is a non-negative constant, $0 \leq \alpha_0 \leq 1$.

$$p = p_0 \quad \text{for } r = a. \quad (13)$$

The solution of the micropolar fluid flow equations (9) subject to the corresponding boundary conditions (10–13) has been obtained by Kucaba-Pietal and Migoun [24]. In this paper, the calculation of the squeezing flow characteristics is based on the explicit analytical formulas for load carrying capacity W_m and the squeeze film time T , which were determined therein. The formula for load supporting capacity W_m reads as follows:

$$W_m = \int_0^a 2\pi r (p - p_0) dr = \frac{\pi U a^4 \mu_N}{8M_1} \quad (14)$$

where

$$\begin{aligned} M_1 &= \frac{1}{6} h^3 + \left[\cosh(mh) \frac{\kappa}{m^2} \right] Y \mu_N + \\ &+ (-\sinh(mh) + mh) \frac{\kappa}{m^2} X \mu_N + h^2 Z \mu_N. \end{aligned} \quad (15)$$

The functions X , Y and Z , and the parameter m , which all appear in the above expressions, are defined as follows:

$$Y = \frac{-Z(1 + 2\alpha_0)}{\alpha_0 \kappa + 1} \quad (16)$$

$$\begin{aligned} X &= (\cosh(mh) - 1)^{-1} \\ &\left[\frac{1 + 2\alpha_0}{\alpha_0 \kappa + 1} Z \sinh(mh) - \frac{mh}{\kappa} \left(2Z + \frac{h^2}{2\mu_N} \right) \right] \end{aligned} \quad (17)$$

$$\begin{aligned} Z &= \frac{-\frac{h}{2\mu_N} + \left[-1 + \coth\left(\frac{mh}{2}\right) \frac{mh}{\kappa} \right] + \alpha \frac{h}{2\mu_N} \left[2 - \coth\left(\frac{mh}{2}\right) mh \right]}{\alpha \left[-\kappa \coth\left(\frac{mh}{2}\right) \frac{1 + \alpha_0}{\alpha_0 \kappa + 1} + \sinh(mh) - 2 \frac{mh}{\kappa} \right]} + \\ &+ \frac{\frac{h}{2\mu_N} \left[-1 + \coth\left(\frac{mh}{2}\right) \frac{mh}{\kappa} \right] + \alpha \frac{h}{2\mu_N} \left[2 - \coth\left(\frac{mh}{2}\right) mh \right]}{-\left[\frac{2\alpha_0 + 1}{\alpha_0 \kappa + 1} (\cosh(mh) + 1) \right] + \left[\frac{\kappa}{\mu_N} \coth\left(\frac{mh}{2}\right) \right]} \end{aligned} \quad (18)$$

$$m = \sqrt{\frac{4\mu_N \kappa}{(2\mu_N + \kappa)\gamma}}. \quad (19)$$

For the case where a Newtonian fluid is squeezed between the plates, load supporting capacity W_N is reduced to:

$$W_N = \frac{3\pi\mu_N U a^4}{2h^3}. \quad (20)$$

The formula for the time T_m taken in reducing the height h_o to a prescribed film thickness h , obtained in the reference [24], reads as follows:

$$T_m = \frac{3\pi\mu_N a^4}{4W} \frac{1}{6} \int_{h_0}^h \frac{dh}{M_1}. \quad (21)$$

The relevant formula for the time T_N to reduce the height h_o of a Newtonian fluid squeezed between the plates is

$$T_N = \frac{3\pi\mu_N U a^4}{4W} \left(\frac{1}{h^2} - \frac{1}{h_0^2} \right). \quad (22)$$

In the paper referred to herein, the above formulas have been expressed in terms of the dimensionless parameters L and N as well.

4. Results and discussion

4.1. Data used for squeeze film characteristics calculation.

Values of experimentally determined micropolar fluid constants for water and the fluids used in defectoscopy [25, 26], and values predicted for water [18] based on molecular dynamic simulations are used in this work. In [25, 26], a method to experimentally determine the parameters characterizing the microstructure of a liquid is proposed. Formulae for the calculation of micropolar viscosity coefficients from the micropolar parameters are given, and the values of the micropolar parameters for water and exemplifying fluids used in defectoscopy are listed. For the calculation of simple flows, for instance the Hagen–Poiseuille flow, the values of the fluid micropolar parameters are sufficient to make accurate predictions. For other, non-simple flows, values of the viscosity coefficients are explicitly needed. To perform the calculations, we assume that $\alpha_o = 0.2$. For water and the three fluids, P1, P2 and P3, as denoted in [25], the coefficients were calculated and are listed in Table 1.

Table 1

Values of micropolar viscosity coefficients for real fluids derived from experimental data and from MD simulations

Fluid/viscosity coefficients	μ 10^{-3} Pa s	κ 10^{-3} Pa s	γ 10^{-21} kg m s ⁻¹
P ₁	2.933	4.824	2.878
P ₂	0.985	1.935	2.607
P ₃	0.636	1.568	1.002
water (1)	0.668	0.214	4.475
water (2) [18]	0.92 +/- 0.09	0.17 +/- 0.03	3.0

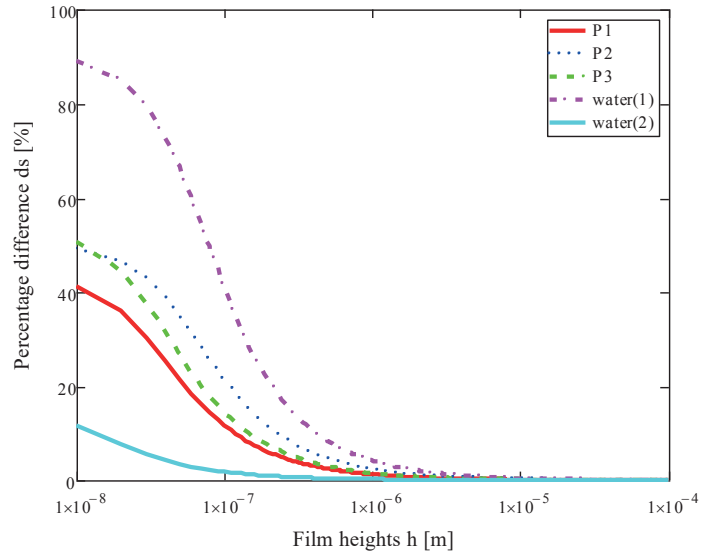


Fig. 2. Percentage difference $ds(h) = W_m(h) - W_N(h)/W_N(h) * 100\%$ in the case of fluids: P₁, P₂, P₃ and water for various film heights h [m]

In the last row of Table 1, the values for water at 16°C are listed, which were evaluated by Hansen et al. [18] using equilibrium molecular dynamics. Determination of the viscosity coefficients of a liquid based on molecular dynamics is a new and highly promising method. However, the results are strongly dependent on the molecular model of water [27]. Variations in the data derived on the basis of different methodologies are small, but we can still observe discrepancies in the values. On the other hand, we should keep in mind that the results of experimental measurements of the micropolar parameters are also subject to errors.

For this reason, the calculations of the squeezing water characteristics were performed twice. All calculations obtained for water using data from [18] are marked in the paper as *water(2)*, while the results derived from experimental data are marked as *water(1)*.

4.2. Load carrying capacity. The load comparison parameter $s(h)$, which is dependent on the gap height h , is defined with the following ratio:

$$s(h) = W_m(h)/W_N(h). \quad (23)$$

The percentage difference of the load calculations, performed using micropolar fluid dynamics (denoted as $W_m(h)$) and classical hydrodynamics (denoted as $W_N(h)$), is given as $ds(h) = W_m(h) - W_N(h)/W_N(h) * 100\%$ and shown in Fig. 2. The difference is observable only for very small values of the film height. For $h = 10^{-6}$ [m], the differences in the results for fluids are as follows: 1.2% for P1, 2.3% for P2, 1.5% for P3, and 4% for *water(1)* as well as 0.3% for *water(2)*. The differences increase with the decrease in film height.

Results from Fig. 2 show that for every fluid beginning from a certain gap height, the load capacity calculated using the micropolar fluid model is larger than the one calculated with the classical Newtonian model of the fluid. More importantly, it

can be observed that every fluid has its “own” value of the limiting gap height, starting from which the load comparison parameter, $s(h)$, begins to increase. The above suggests that the value depends on rheological properties of the fluid – values of the micropolar viscosity coefficients.

Let us now examine the effect observed in detail in terms of the microstructural parameters L and N . For the fluids under consideration, the values of parameters N and l (8) were obtained using data from Table 1 and are listed in Table 2. Relevant formulas for load capacities W_m and W_N , expressed by L and N , which were previously derived in [24], were used for calculations of $s(L, N)$.

Table 2
 Dimensionless parameter values l and N for fluids P1, P2, P3 and water

	P1	P2	P3	water(1)	water(2)
L	0.036	0.062	0.041	0.099	0.0866
N	0.558	0.577	0.589	0.689	0.367

Figure 3 illustrates the dependence of the load comparison parameter $s(L, N)$ on L with $L_c = h$ in (8). It can be observed that the $s(L, N)$ value is strongly affected by parameters N and L , and $s(L, N)$ increases when L decreases starting from the value of $L = 10000$, which is common for all of the fluids under consideration.

These results indicate that for the parameter value $L < 10000$ (i.e. $h < 10^4 l$), the micropolar effects in the fluid increase the load capacity calculations, and should be performed using the micropolar fluid model. The micropolar effect is negligible above this value; therefore, it is worthwhile to carry out load calculations based on classical hydromechanics, which is considerably simpler than the micropolar fluid theory.

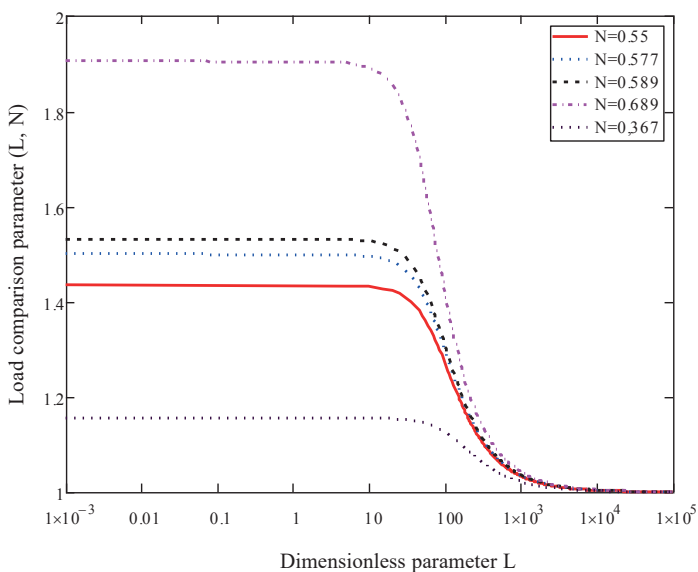


Fig. 3. Dependence of the load comparison parameter $s(L, N)$ on L for fluids P1 ($N = 0.558$), P2 ($N = 0.577$), P3 ($N = 0.589$), and water(1) ($N = 0.689$) and water(2) ($N = 0.367$)

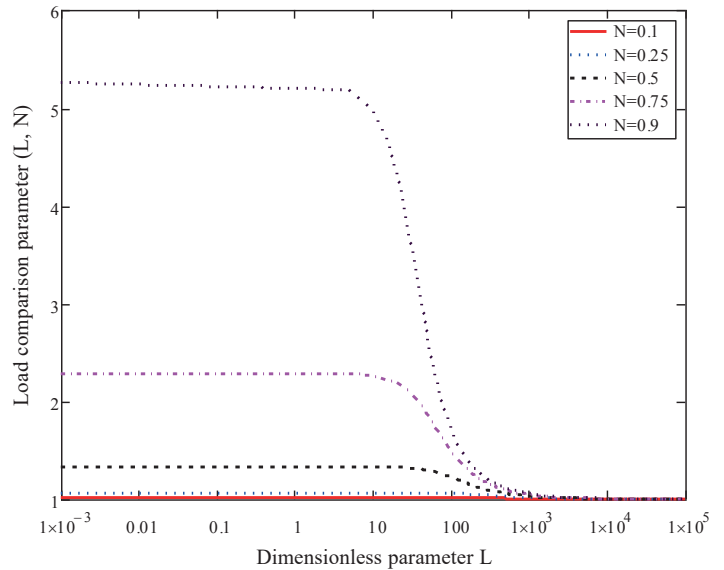


Fig. 4. Dependence of load comparison parameter $s(L, N)$ on L for some “artificial” fluids characterized by different values of N

From data presented in Table 3, which summarizes some of the results of the calculations performed, we can observe that when $L = 10000$, the value of s is always less than 1.004, and when $L = 1000$, the value of s is smaller than 1.04. This means that the percentage difference in the calculation results obtained based on both fluid models does not exceed the value of 0.4% for $L = 10000$ and 4% for $L = 1000$.

Table 3
 Load comparison parameter $s(L, N)$ for various values of L in the case of fluids P1, P2, P3 and water

	P1	P2	P3	water(1)	water(2)
$L = 10000$	1.003	1.003	1.004	1.004	1.002
$L = 1000$	1.033	1.035	1.035	1.042	1.021
$L = 100$	1.27	1.296	1.308	1.417	1.126

Using the values of l from Table 2, we are now able to calculate the particular limiting value of the gap height h for a given fluid, starting from which the difference between the load-bearing capacity calculations performed on the basis of both fluid models is less than the desired accuracy, i.e. 0.4%. For each of the fluids under consideration, the h value in [m] is equal to: $3.6 \cdot 10^{-6}$ for P1, $6.2 \cdot 10^{-6}$ for P2, $4.1 \cdot 10^{-6}$ for P3, and $9.9 \cdot 10^{-6}$ (water(1)) and $8.6 \cdot 10^{-6}$ (water(2)) for water. The results obtained using the dimensionless parameter values from Table 2 match the estimates presented in Figs. 3 and 4.

To study the effects of parameter N on $s(L, N)$ for a wide range of N values, calculations were performed for “artificial” fluids characterized by different values of parameter N , and the results are presented in Fig. 4.

We can see that an increase in the value of parameter N (with constant L) results in an increase in the value of $s(L, N)$.

For instance, for $L = 0.01$, the load bearing capacity is more than five times larger for a fluid characterized by parameter $N = 0.9$ than for a fluid characterized by parameter $N = 0.1$. Moreover, a decrease in the value of parameter L increases the load comparison parameter $s(L, N)$ value, starting from $L < 10000$. These results allow for predicting the value of h between approaching plates for each fluid inside of a gap, if only their L and N parameters values are known, in the same way as it was performed above for real fluids.

4.3. Squeeze film time. The time required for reducing the initial film thickness $T_m(h)$ from h_o to h was calculated with the micropolar model of the fluid in the gap using equation (21), and compared to the corresponding reducing time $T_N(h)$ calculated with the Newtonian fluid model, according to equation (22). The value of h_o was assumed to be $h_o = 10^{-3}$ [m]. The squeeze film time comparison parameter $T(h)$ is defined as the following ratio:

$$T(h) = T_m(h)/T_N(h). \quad (24)$$

The percentage difference is given as $dt(h) = (T_m(h) - T_N(h))/T_N(h) * 100\%$ and is depicted versus h in Fig. 5. The results show that the decreasing values of the gap height increase the squeezing time as compared to the Newtonian case, starting from the limiting film height, the value of which is characteristic for each fluid. The difference dt increases with the decrease in the film height and for $h = 10^{-6}$ [m] their values are as follows: 0.79% for P1, 1.52% for P2, 0.97% for P3, and 2.47% (*water(1)*) and 0.12% (*water(2)*) for water. When the film height is smaller, i.e. $h = 10^{-7}$ [m], the dt differences increase to: 7.8% for P1, 14.65% for P2, 9.68% for P3, and 27.8% (*water(1)*) and 1.2% (*water(2)*) for water.

We can observe that for a fixed value of h for a given fluid, the value of the squeeze time comparison parameter $T(h)$ is

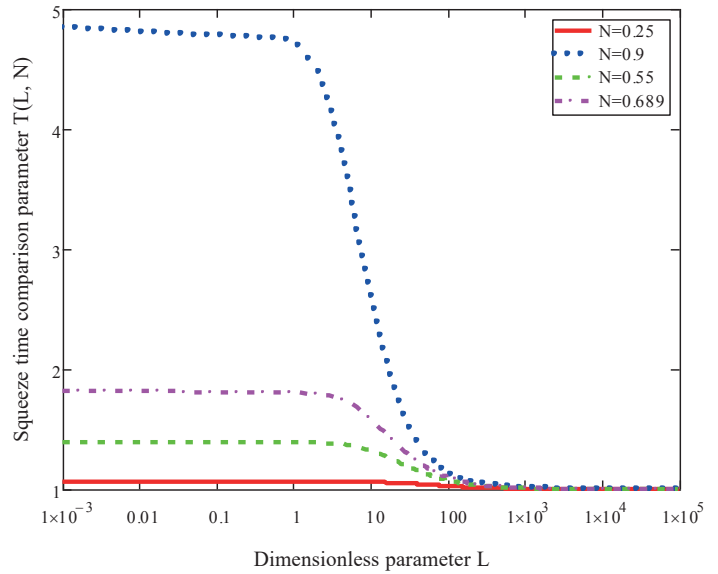


Fig. 6. Squeeze time comparison parameter $T(L, N)$ as a function of L for fluids P1 ($N = 0.55$), *water(1)* ($N = 0.89$) and two artificial fluids with values of parameter $N = 0.25$ and $N = 0.9$

slightly lower than the load comparison parameter $s(h)$. The results of the calculations of the squeeze film time comparison parameter $T(L, N)$, dependent on parameters L and N , are depicted in Fig. 6.

To illustrate the dependence on a wider scale of N , data for P1, *water(1)* and two artificial fluids characterized by values $N = 0.25$ and $N = 0.9$ are presented in Fig. 6. When analyzing the results, it can be concluded that the $T(L, N)$ value is strongly affected by parameters N and L . For $L > 10000$ (i.e. $h < 10^4 l$), the value of $T(L, N) = 1$, otherwise $T(L, N) > 1$.

An increase in the value of parameter N (with constant L) results in an increase in the value of T . For instance, the squeeze film time is almost five times greater for fluids characterized by $N = 0.9$ than for fluids with $N = 0.25$.

5. Conclusions

In this paper, an analysis of the impact of scale on MFT modeling for squeezing flow was performed. According to the results obtained, the following conclusions can be formulated.

- The maximum distance between plates, h , for which the fluid film micropolar effect enhances the values of load carrying capacity and lengthens the approaching time of the parallel plates can be defined by the fluid micropolar constants as $h_{max} = 10^4 (\gamma / (4\mu + 2\kappa))^{1/2}$, or expressed by micropolar dimensionless parameters (defined in equation (8)) as $L_{max} = 10000$.
- For distances greater than $h > h_{max}$, the calculations of the squeeze film characteristics between flat parallel plates for both the micropolar fluid and the Newtonian fluid models are the same (i.e. discrepancies in values are lower than 1%),

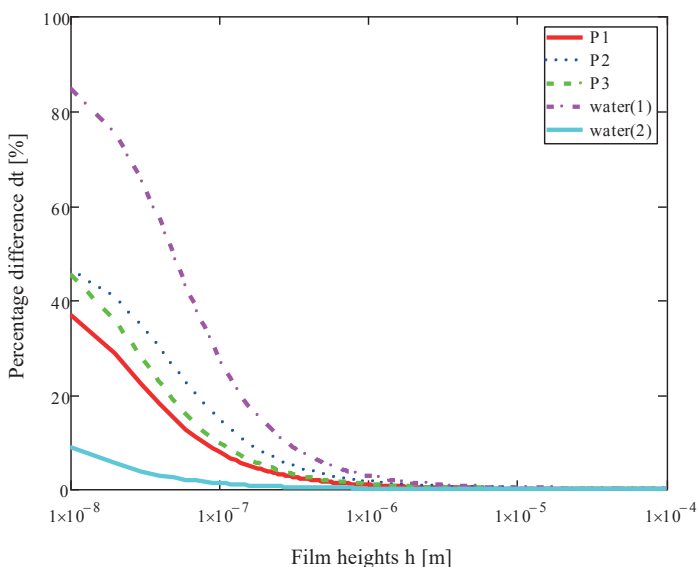


Fig. 5. Percentage difference $dt(h)$ as a function of film height h in the case of fluids P1, P2, P3 and water

- Only for $L < 10000$ the load carrying capacity and the squeeze film approximation time calculated based on MFT are greater, as compared to the classical case, i.e. using the Newtonian fluid model.
- For Hagen–Poiseuille flow characteristics, the above inequality counterpart has the following form: $L < 10000$ [15], i.e. the maximum geometrical dimension of the flow field for which the fluid micropolar effects are negligible is ten times lower for squeeze flow than its counterpart for the Hagen–Poiseuille flow.
- The above analysis gives an answer to the fundamental question, which appeared during microflows research, of why the results obtained using of classical hydrodynamics equations, with regard to the flows of the same real fluid, are in agreement with the experiment on one occasion and disagree with it on another one. For distances lower than h_{max} , the micropolar fluid model is most suitable, for distances larger than h_{max} it is more effective to carry on the calculations on the basis of classical dynamics, i.e. Navier–Stokes equations, which are simpler than those of micropolar fluid flow.

REFERENCES

- [1] D.F. Hays, “Squeeze films for rectangular plates”, *J. Fluids Eng.* 85 (2), 243–246 (1963).
- [2] B.J. Hamrock, *Fundamental of Fluid Film Lubrication*, New York, McGraw-Hill, 1994.
- [3] J. Prakash, P. Sinha, “Cyclic squeeze films in micropolar fluid lubricated journal bearing”, *ASME J Tribol.* 98 (3), 412–417 (1976).
- [4] J. Prakash, P. Sinha, “Squeeze film theory for micropolar fluids”, *ASME J. Lubr. Technol.* 98 (1), 139–144 (1976).
- [5] O.A. Bég, M.M. Rashidi, T.A. Bég, M. Asadi, “Homotopy analysis of transient magneto-bio-fluid dynamics of micropolar squeeze film in a porous medium: a model for magneto-biorheological lubrication”, *Journal of Mechanics in Medicine and Biology* 12 (3), 1–21 (2012).
- [6] M.E. Shimpi, G.M. Deheri, “Magnetic fluidbased squeeze film performance in rotating curved porous circular plates: the effect of deformation and surface roughness”, *Tribology in Industry* 34 (2), 57–67 (2012).
- [7] X. Wang, K.Q. Zhu, “Numerical analysis of journal bearings lubricated with micropolar fluids including thermal and cavitating effects”, *Tribol Int* 39 (3), 227–237 (2006).
- [8] A. Siddangouda, “Squeezing film characteristics for micropolar fluid between porous parallel stepped plates”, *Tribology in Industry* 37 (1), 97–106 (2015).
- [9] A.C. Eringen, “Theory of micropolar fluids”, *J. Math. Mech.* 16, 1–16 (1966).
- [10] S. Ram, “Numerical analysis of capillary compensated micropolar fluid lubricated hole-entry journal bearings”, *Jurnal Tribologi* 9, 18–44 (2016).
- [11] N. Ram and S.C. Sharma, “Influence of micropolar lubricants on asymmetric slot-entry journal bearing”, *Tribology Online* 10(5), 320–328 (2015).
- [12] N. Ram, S.C. Sharma, and A. Rajput, “Compensated hole-entry hybrid journal bearing by CFV restrictor under micropolar lubricants”, *Proceedings of Malaysian International Tribology Conference*, 171–172 (2015).
- [13] D.C. Rapaport, “Shear-induced order and rotation in pipe flow of short-chain molecules”, *Europhysics Letters* 26 (6), 401–406 (1994).
- [14] J. Delhommelle, D.J. Evans, “Poiseuille flow of micropolar fluid”, *Molecular Physics*, 100 (17), 2857–65 (2002).
- [15] A. Kucaba-Pietal, *Microflows Modelling by Use Micropolar Fluid Theory*, OW PRz, Rzeszów, 2004 (in Polish).
- [16] A. Kucaba-Pietal, “Microchannels flow modelling with the micropolar fluid theory”, *Bull. Pol. Ac.: Tech.* 52 (3), 209–214 (2004).
- [17] A. Kucaba-Pietal, Z. Peradzyński, Z. Walenta, “MD Computer simulation of water flows in nanochannels”, *Bull. Pol. Ac.: Tech.* 57(1), 1–7 (2009).
- [18] J.S. Hansen, H. Bruus, B.D. Todd, P. Daivis, “Rotational and spin viscosities of water: Application to nanofluidics”, *Phys. Review E* 84, 036311 (2011).
- [19] G. Łukaszewicz, *Micropolar Fluids. Theory and Application*, Birkhouser, Berlin, 1999.
- [20] J. Badur, P.J. Ziółkowski, P. Ziółkowski, “On the angular velocity slip in nano-flows”, *Microfluid Nanofluid* 19, 191–198 (2015). doi 10.1007/s10404–015–1564–6
- [21] M. Ghanabi, S. Hossainpour, G. Rezazadeh, “Study of squeeze film damping in a micro-beam resonator based on micropolar theory” (2015). <http://dx.doi.org/10.1590/1679-78251364>
- [22] K.A. Kline, S.J. Allen, “Nonsteady flows of fluids with microstructure”, *Physics of Fluids* 13, 263–283 (1970).
- [23] A.J. Willson, “Basic flows of micropolar liquid”, *Appl. Sci. Res.* 20, 338–335 (1969).
- [24] A. Kucaba-Pietal, N.P. Migoun, “Effects of non-zero values of microrotation vector on the walls on squeeze film behaviour of micropolar fluid”, *Intern. J. Nonl. Sci. and Num. Sim.* 2 (2), 115–127 (2001).
- [25] P. Prokhorenko, N.P. Migoun, M. Stadthaus, *Theoretical Principles of Liquid Penetrant Testing*, DVS Verlag, Berlin, 1999.
- [26] V.S. Kolpashchikov, N.P. Migoun, P. Prokhorenko, “Experimental determination of material micropolar fluid constants”, *Int. J. Engng. Sci.* 21 (4), 405 (1983).
- [27] A. Kucaba-Pietal, “Nanoflows modelling”, in *Nanomechanics. Selected Problems*, (eds. A. Muc, M. Chwał, A. Garstecki, G. Szefer), Wydawnictwo PK, Kraków, 51–62 (2014).
- [28] A.P. Markensteijn, R. Hartkamp, S. Lunding, J. Westerweel, “A comparison of the value of viscosity for several water models using Poiseuille flow in a nano-channel”. *J. Chem. Phys.* 136, 134104 (2012). doi 10.1063/1.3697977